PHILOSOPHICAL TRANSACTIONS OF THE ROYAL SOCIETY A MATHEMATICAL, PHYSICAL & ENGINEERING SCIENCES

Structure and Bonding in the Deep Mantle and Core

Russell J. Hemley and Ronald E. Cohen

Phil. Trans. R. Soc. Lond. A 1996 **354**, 1461-1479
doi: 10.1098/rsta.1996.0058

Structure and bonding in the deep mantle and core

By Russell J. Hemley and Ronald E. Cohen

Geophysical Laboratory and Center for High-Pressure Research, Carnegie Institution of Washington, 5251 Broad Branch Rd NW, Washington, DC 20005-1305, USA

Recent high-pressure experimental and theoretical studies provide growing evidence for fundamental changes in bonding properties of many materials under deep Earth conditions. The crystal chemistry of materials at high pressure, especially those containing open-shell elements such as Fe, can differ markedly from that at low pressure and in low-pressure phases. On the other hand, concepts such as transferable ionic radii and coordination polyhedra, which are useful for describing structure and bonding in low-pressure phases, can be successfully applied to some systems (e.g. those containing closed shell ions) if effects of ion compression and orbital hybridization are taken into account. Recent results for simple oxides, silica, perovskites and metals to mantle and core pressures and temperatures are briefly examined.

1. Introduction

Since the early days of mineralogy, the interaction between theory and experiment has formed the underpinning of our view of structure and bonding in Earth materials. Goldschmidt (1926) systematized the concept of transferable ionic radii on the basis of extensive studies of crystal structure with the then-new X-ray diffraction technique. This concept was immediately refined and put on a theoretical footing by Pauling (1927) using the just-developed techniques of quantum mechanics. This, in its modern variants (see, for example, Shannon & Prewitt 1981), has become the basis for many empirical schemes for predicting structure and bonding patterns in minerals, for example using polyhedral modelling techniques (see, for example, Hazen & Finger 1984). Thus, the principles of structure and bonding in minerals of the near-surface environment are now quite well understood experimentally and theoretically (see, for example, Pauling 1960; O'Keeffe & Navrotsky 1981; Bukowinski 1994).

Minerals undergo a wide degree of compression over the pressure range of the lower mantle ($\Delta V/V_0$ to 30%, 23–135 GPa) and core ($\Delta V/V_0$ to 50%, 135–364 GPa), and investigation of the effects of such high pressures on mineral structure has a long history. Central to this issue from the viewpoint of ionic models is the concept of increasing cation and anion coordination, and the concomitant tendency toward close-packing, with pressure (Hazen & Finger 1984). In addition, significant changes in electronic properties, which go beyond the ken of conventional ionic models are also possible. Under extreme pressure conditions, the orbital structure of the component ions (or atoms) and the associated valency characteristic of chemical bonding

Phil. Trans. R. Soc. Lond. A (1996) **354**, 1461–1479
Printed in Great Britain

at low compressions are lost as a result of the increase in electronic kinetic energy (giving rise ultimately to a plasma state at the highest compressions). Under these conditions, the energetics and other properties of highly compressed materials have been described by Thomas–Fermi–Dirac-type models, which neglect such chemical effects and by their nature are relatively crude at low pressures but become exact with increasing density (see, for example, Elsasser 1951). The extent to which these conditions are approached deep within the Earth and terrestrial planets has been a crucial question since the early days of mineral physics. More generally, the recognition of the potentially large perturbations of pressure on minerals suggests a need to examine carefully the evolution in bonding properties of such materials with increasing depth within planets.

As a result of recent breakthroughs in high-pressure techniques, accurate studies of structure and related properties of minerals can now be performed under conditions of the deep mantle and core (see, for example, Mao & Hemley and other papers in this volume). In addition, theoretical methods have improved considerably and are able to make highly accurate predictions (see, for example, Bukowinski 1994). Taken together, experiment and materials theory provide new insights that in many cases are not evident when results from either approach are examined separately. The major finding of this work is the growing evidence for fundamental changes in bonding properties of many materials under deep Earth conditions. Iron assumes a critical role in mantle phases, for example, and recent experiments are providing compelling evidence that its behaviour (e.g. crystal chemistry) at very high pressures differs markedly from that at low pressure and in low-pressure phases. This paper examines structure and bonding in deep mantle and core materials using experimental and theoretical results. We examine the applicability of rules developed to describe bonding properties in low-pressure mineral phases. We do this by describing a few key examples; in particular, recent studies of oxides, silica, perovskites and metals under deep Earth conditions.

2. Examples

(*a*) MgO

The alkaline-earth oxides have long been recognized as models for the behaviour of oxides at high pressure. Polymorphism in MgO, as well as the heavier alkaline-earth oxides, has been an important testing ground for theory. Both CaO and SrO transform from the B1 to B2 structure under pressure, observations that can be reproduced by both approximate theoretical models as well as being consistent with first-principles results (see, for example, Mehl *et al.* 1986, 1988). No such transition has yet been observed in MgO. Recently, synchrotron X-ray diffraction measurements on MgO have demonstrated that the B1 structure is stable at room temperature to at least 227 GPa, i.e. to pressure well in excess of the lower mantle (Duffy *et al.* 1995). These results also provide a highly accurate equation of state (figure 1). In this work, it was necessary to take into account the effect of non-hydrostatic stresses on the measured volume.

The experimental results are in excellent agreement with a number of first-principles calculations. The results are consistent with the wide field of stability predicted for the B1 structure; e.g. linearized augmented plane wave (LAPW) calculations predict a transition pressure of 500 GPa (Mehl *et al.* 1988). There is also good agreement between theory and experiment for the equation of state; figure 1

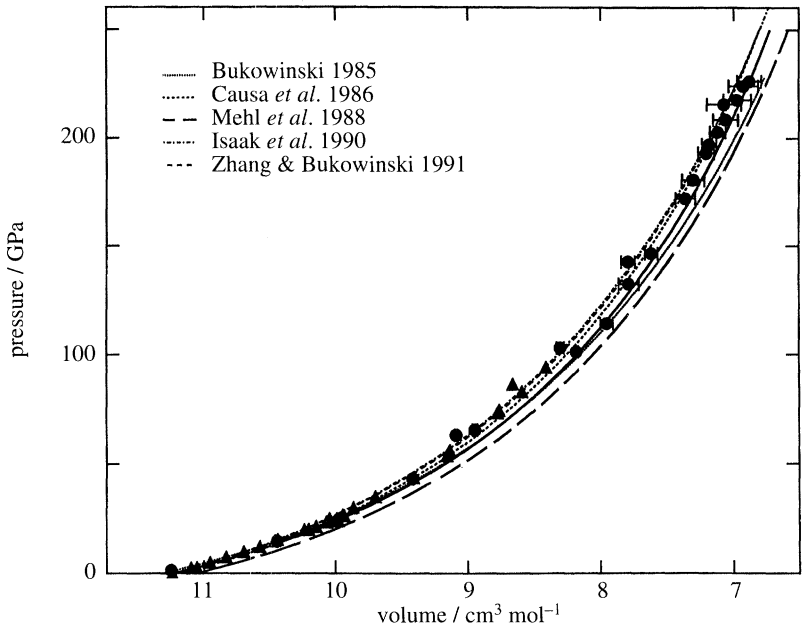

Figure 1. Pressure-volume equation of state for MgO. The bold solid line is the hydrostatic compression curve (Duffy *et al.* 1995). Data points: circles are diamond-cell results uncorrected for non-hydrostatic stresses; triangles are earlier static and shock-wave results.

compares static and shock-derived room-temperature compression curves with several theoretical calculations (Bukowinski 1985; Causa *et al.* 1986; Mehl *et al.* 1988; Isaak *et al.* 1990; Zhang & Bukowinski 1991). The calculated charge density reveals well-defined ions having a largely spherical shape, as shown in figure 2 which is from the LAPW calculation of Mehl *et al.* (1988). At extreme pressures, the charge density contours for Mg become cubic. Theory thus shows that MgO is essentially perfectly ionic (well described as consisting of Mg^{+2} and O^{-2} ions) over a wide range of pressures; this is illustrated in the difference density plot shown in figure 3. Although the material is ionic, it is inappropriate to consider the material as consisting of rigid ions (fixed ionic radii). The effective size of the O^{-2} ion extends well past the neighbouring Mg^{+2} spheres, and the size of the ion is responsive to its environment. The simplest consequence of this is that the Cauchy condition for central pairwise forces ($C_{12} - C_{44} = 2P$) is not obeyed (Mehl *et al.* 1986). Simple non-empirical models that allow for spherical charge relaxation of the O^{-2} ions give the correct behaviour (Mehl *et al.* 1986; Wolf & Bukowinski 1988; Isaak *et al.* 1990; Inbar & Cohen 1995).

With these non-empirical ionic model techniques, it is possible to calculate thermal and elastic properties over a wide range of conditions, including those beyond the P–T range of existing measurements. Thermoelastic properties, such as the thermal expansivity α and Anderson–Grüneisen parameter $\delta_T = (\ln \alpha / \ln V)_T$ calculated from lattice dynamics and molecular dynamics from non-empirical ionic models are also in good agreement with experimental measurements (see, for example, Isaak *et al.* 1990; Inbar & Cohen 1995). Another important geophysical parameter is ν, which is defined as $\mathrm{d}\ln v_S / \mathrm{d}\ln v_P$. Seismic data indicate values of this parameter in the lower mantle of greater than 2, which has been difficult to understand on the basis of low-pressure elasticity data. Calculations for MgO show that such high values are expected at high P–T conditions in oxides and are associated with the pressure-

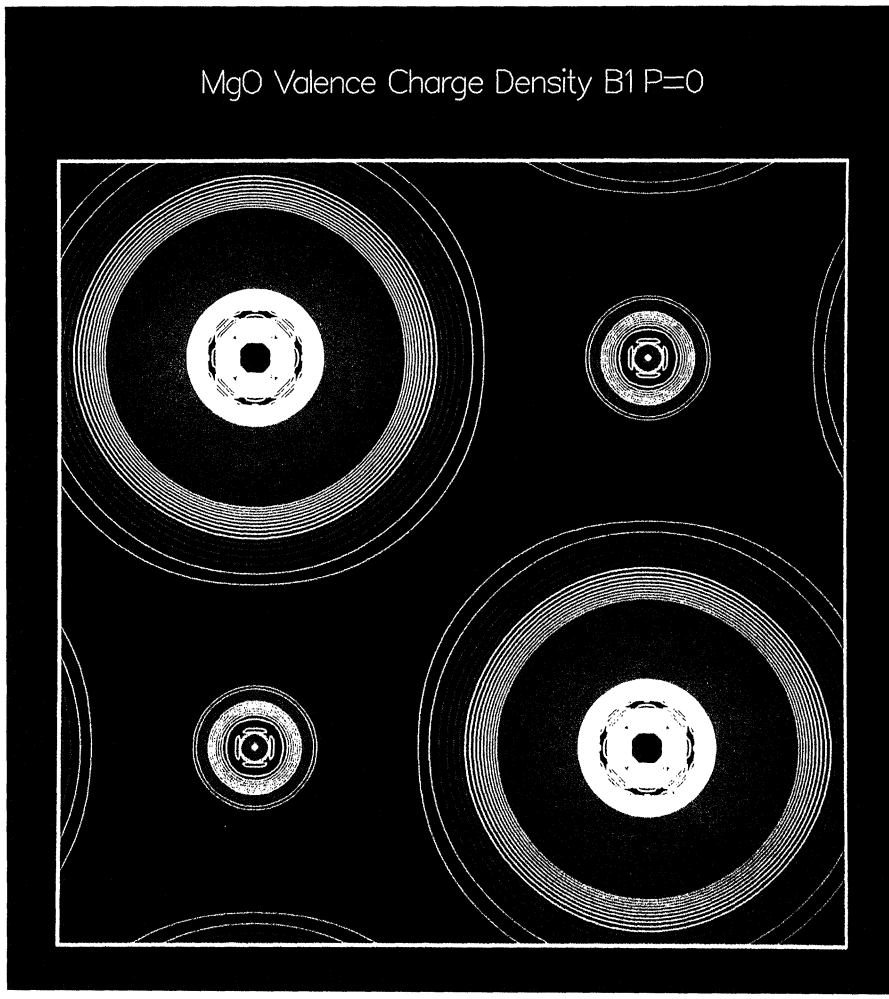

Figure 2. Calculated valence charge density contours for MgO in the B1 structure. (*a*) 5 GPa. (*b*) 754 GPa (Mehl *et al.* 1988). Only the O 2p states are shown. The contours correspond to 0.01 electrons bohr^{-3}. There is little valence charge on the Mg because of the highly ionic character of the material. However, MgO becomes less ionic at extreme conditions where more overlap is observed theoretically (*b*). In the higher pressure calculation, the B1 structure is metastable with respect to B2. Copyright American Geophysical Union.

induced decrease in δ_T and increase of K/G, where K is the bulk modulus and G is the shear modulus (Isaak *et al.* 1992). In addition, the experimental evidence for a change in the sign in elastic anisotropy under pressure (Duffy *et al.* 1995) was predicted theoretically (Isaak *et al.* 1990). These calculations for MgO thus provide an important benchmark for other materials.

(*b*) FeO

Owing to the open shell character of iron, FeO has a more complicated electronic structure and chemistry, and its behaviour under pressure has received considerable attention recently. The B1–B2 transition has been predicted theoretically for FeO but is apparently occluded experimentally by transitions to lower symmetry structures.

PHILOSOPHICAL TRANSACTIONS OF THE ROYAL SOCIETY A MATHEMATICAL, PHYSICAL & ENGINEERING SCIENCES

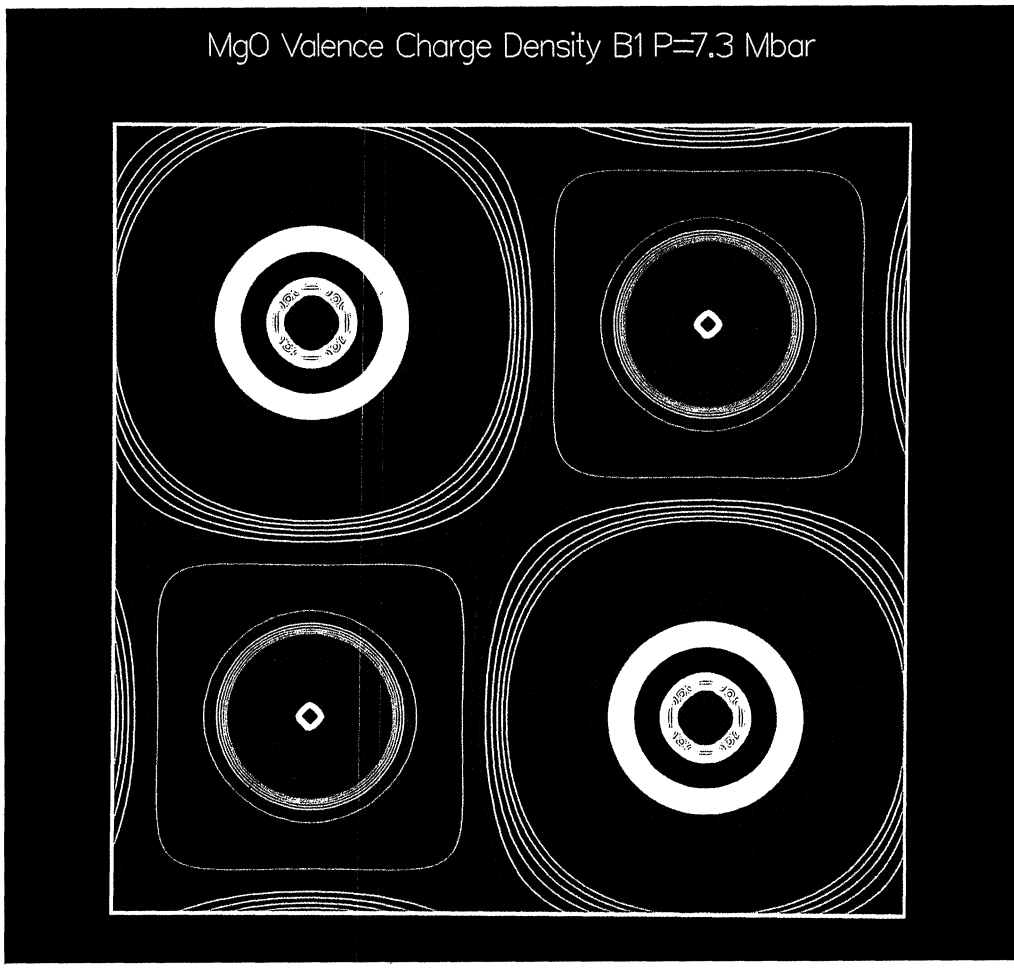

Figure 2. *Cont.*

Whereas MgO remains in the B1 structure to pressures well in excess of those of the lower mantle, FeO undergoes a rhombohedral distortion at about 17 GPa (Mao *et al.* 1996). At the transition, the low-pressure face-centred cubic (FCC) crystal of wüstite distorts reversibly to a rhombohedral structure by elongation of a body diagonal (111) and contraction of the other three body diagonals. The elongated diagonal becomes the c-axis of a rhombohedral cell, with the distortion increasing with pressure. The transition is highly sensitive to non-hydrostatic stresses. In a uniaxial compression experiment, an unprecedented large systematic variation of the c/a ratio (up to 10%) as a function of orientation was observed in the rhombohedral phase. The results have resolved a long-standing paradox concerning the high-pressure equation of state and phase transition in this material.

The microscopic origin of the transition may be gleaned from electronic structure calculations. The pressure dependences of the rhombohedral strain and the calculated magnetic moment are shown in figure 4. Theory overestimates the strain, although the volume dependence is quite close (Isaak *et al.* 1993). Moreover, these calculations also show a significant change in magnetic properties with pressure (calculated for

PHILOSOPHICAL TRANSACTIONS OF THE ROYAL SOCIETY A MATHEMATICAL, PHYSICAL & ENGINEERING SCIENCES

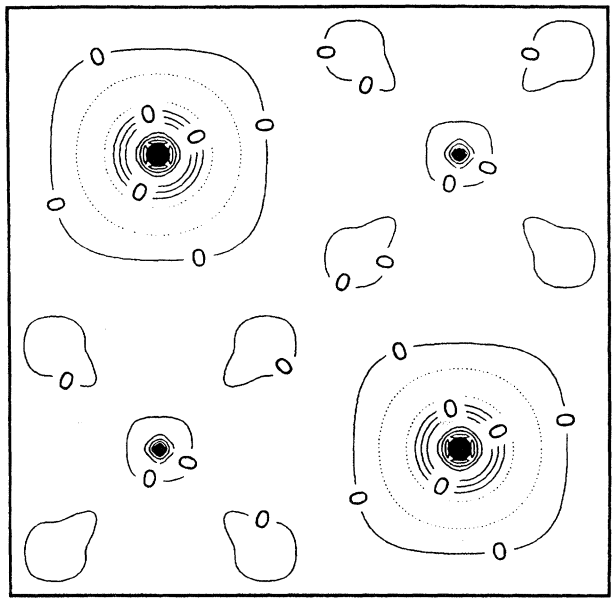

Figure 3. Difference charge density map for MgO comparing the fully self-consistent results from LAPW calculations (Mehl *et al.* 1988) with the potential-induced breathing (PIB) model (Isaak *et al.* 1990). At zero pressure, MgO is perfectly ionic and is represented well by overlapping Mg^{+2} and O^{-2}. The only differences from the self-consistent charge density are the orthogonalization spikes found near the nuclei. Contour levels are 0.005 electrons $bohr^{-3}$.

B1 and B2 structures; Isaak *et al.* 1993). The difference charge density map, in which the electron density calculated from the ionic model is subtracted from that determined from a fully self-consistent local density approximation calculation, is shown in figure 5. These results indicate that the rhombohedral distortion is driven by development of metal–metal bonding planes, as shown by the red areas which identify regions of excess electron density.

Several years ago, evidence for a higher P–T transition was discovered by shock-wave techniques (Jeanloz & Ahrens 1980). However, the structure remained unknown. This was recently resolved using the resistively heated diamond cell (Fei & Mao 1994). These experiments revealed a transformation when polycrystalline FeO was compressed to 74 GPa and heated to 900 K. The X-ray diffraction pattern of the high P–T phase is consistent with the hexagonal NiAs structure, as suggested by Navrotsky & Davies (1981) and Jackson & Ringwood (1981). The rhombohedral-NiAs phase boundary has a negative Clapeyron slope of -0.051 GPa K^{-1}, and the B1–NiAs boundary is nearly vertical. There is also evidence that the high P–T phase is metallic (Knittle & Jeanloz 1986); in addition, all metal oxides having the NiAs structure are metallic (see also Sherman 1991; Fei & Mao 1994; Sherman & Jansen 1995). At the core–mantle boundary, the metallic oxide alloy is thus expected to readily form with the metallic iron in the core, and this may control the Fe–Mg ratio of other mantle phases (magnesiowüstite and perovskite).

Understanding the electronic structure of FeO and other transition metal monoxides is currently an active field of condensed-matter research. The problem is that the most commonly used and generally accurate theoretical methods give metallic behaviour for FeO, yet it is known to have a large band gap. Most agree that this failure arises from the inadequacy of the local density approximation (and related

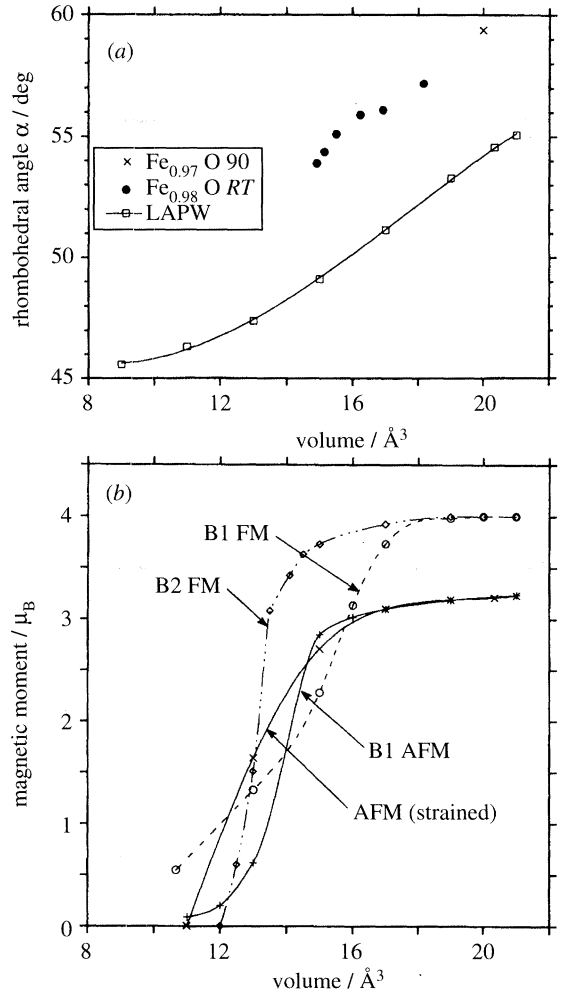

Figure 4. Pressure dependence of the (*a*) rhombohedral strain and (*b*) predicted magnetic moment for FeO (Isaak *et al.* 1993 and references therein). About half of the difference in predicted strain is due to the non-stoichiometry of the experimental samples. The magnetic moment is predicted to drop precipitously at high pressures, giving a high-spin/low-spin transition.

techniques) due to the derivation of the exchange-correlation functional to optimize energies rather than potentials, the neglect of orbitally dependent correlation effects, and/or approximations to the exchange potential. Many models have been proposed to overcome these problems, but none has yet been developed to provide accurate predictions of the band gap as well as energetics as functions of pressure.

(*c*) SiO_2

Silica is produced in chemical reactions in the mantle, possibly in the D″ region. Interest in free silica also arises from the possibility of a silica-enriched lower mantle relative to the upper mantle (Stixrude *et al.* 1992). Figure 6 shows valence charge density iso-surfaces from LAPW calculations (Cohen 1991) for stishovite, rutile-structured SiO_2, where the Si atom is coordinated by six oxygens. This is considered a fairly ionic material, but it does exhibit some covalency, as indicated by the aspherical

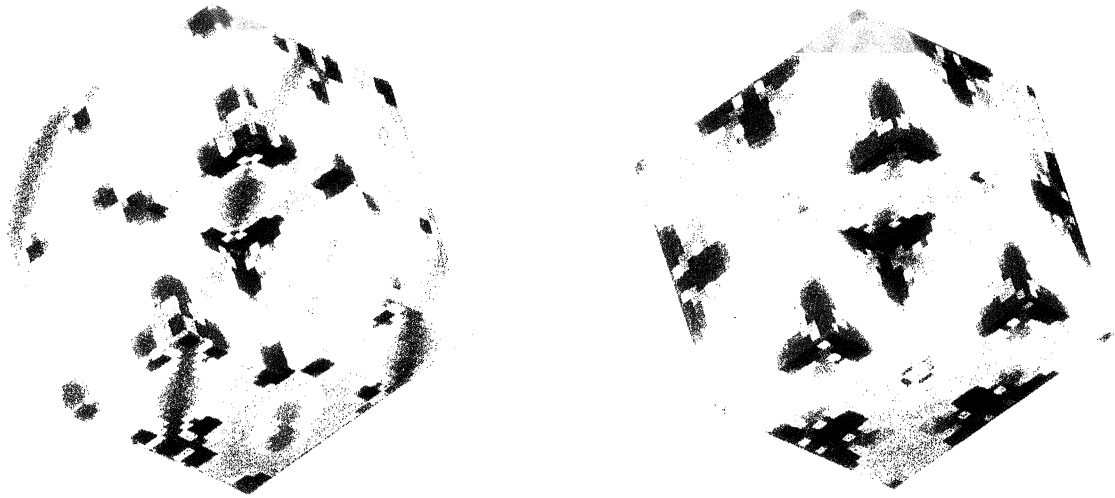

Figure 5. Difference charge density map for FeO between LAPW and PIB calculations. (*a*) Cubic (B1). (*b*) Rhombohedral strain (from Isaak *et al.* 1993). The Fe atoms are located at the centre of the cube and at the cube edges, and the O atoms are on the faces and corners. The red regions show excess charge relative to the spherical ions and the blue regions are deficient in charge. In the strained structure, there is pronounced metal–metal bonding shown by the red bands. Copyright Ronald E. Cohen.

shape of the oxygen charge (polarized towards the Si) and the valence charge on the Si. Note that the oxygen ions are not arrayed in a close packed structure. Compression measurements show an increase in anisotropy with pressure (see Hemley *et al.* 1994). Stishovite is more compressible in the *a* relative to the *c* direction as the result of significant Si–Si repulsion across the shared edges of octahedra that form chains along the *c*-axis. However, the effect of Si–Si repulsion is reduced somewhat by shortening of the O–O distance along the octahedral shared edges. The O–O distance of 2.29 Å is one of the shortest found in any oxide not containing hydrogen. In contrast to the tetrahedral forms of silica, the Si–O distances in stishovite change significantly as pressure is increased from ambient to 15 GPa. Not surprisingly, the equatorial Si–O bonds (involving the shared edges) are less compressible than the apical Si–O bonds that are normal to the *c* direction. Compression is also accommodated by decreases in the O–O distances, but neither the O–Si–O nor the Si–O–Si angles show significant changes with pressure.

Early crystal chemical arguments suggested that the tetragonal structure should become unstable with respect to an orthorhombic distortion to the $CaCl_2$ structure. There is a close relationship between the rutile and $CaCl_2$ structure; the two are related by a simple rotation of octahedra, or a shear in the structure having the same symmetry as the B_{1g} Raman mode. Thus, the transition should be accompanied by a softening of a Raman-active vibration. The soft Raman mode was confirmed by Hemley (1987). The first experimental evidence for the existence of the $CaCl_2$-structured phase was provided by Tsuchida & Yagi (1989) who found a shift of one of the diffraction lines near 100 GPa. On the other hand, LAPW calculations predicted the transition to $CaCl_2$ at the much lower pressure of 45 GPa (Cohen 1992). The transition occurs when C_{11}–C_{12} goes to zero, with the B_{1g} mode vanishing at higher pressures, around 75 GPa, if the rutile symmetry were maintained. The calculations predict that the transition is characterized by a reversal in the pressure shift of the

PHILOSOPHICAL TRANSACTIONS OF THE ROYAL SOCIETY A MATHEMATICAL, PHYSICAL & ENGINEERING SCIENCES

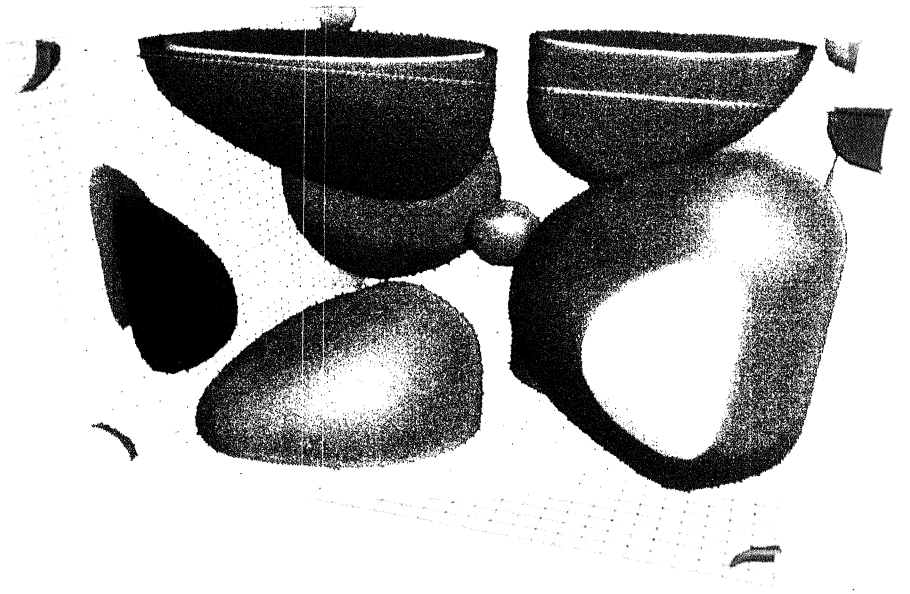

Figure 6. Valence charge density surface for stishovite (from Cohen 1991, 1994). Two iso-density surfaces corresponding to 0.06 and 0.08 electrons bohr^{-3} are shown. Copyright Ronald E. Cohen.

soft B_{1g} mode (in the rutile structure) to the hard A_g mode (in $CaCl_2$); i.e. the B_{1g} correlates with the A_g mode across the transition. Further, the stishovite E_g mode splits into the $CaCl_2$ B_{2g} and B_{3g} at the transition. This prediction has recently been confirmed by higher pressure Raman scattering measurements (figure 7), which find the transition at 50 GPa (Kingma *et al.* 1995). Subsequent single-crystal X-ray diffraction measurements also support the lower transformation pressure (Mao *et al.* 1994). The difference in transition pressure between the new results and the earlier powder X-ray diffraction can be attributed to non-hydrostatic stresses in the latter; in fact, the volume compression at which the transition occurs is similar for the two studies. Ionic models have great difficulty accurately reproducing the properties of stishovite, especially with regard to the rutile-to-$CaCl_2$ transition (see Cohen 1994; Matsui & Tsuneyuki 1992). An important bonding feature for the relative stability of rutile and $CaCl_2$-structured silica is π-bonding, which governs the motions of O out of the Si plane (Burdett 1985; Cohen 1994).

A growing body of data demonstrates that structure and bonding of amorphous SiO_2 changes markedly under pressure and in many ways parallels that observed in the crystalline phases. These results have important implications for the properties (e.g. densities) of silicate melts at deep mantle conditions. *In situ* spectroscopic studies first revealed large structural changes, in silica glass under pressure, including evidence for the increase in coordination in Si (see Hemley *et al.* 1994). More recently, new X-ray diffraction techniques have been applied to study directly these structural changes. From measurements of the structure factor, we obtain the radial distribution function, the first peak of which is the Si–O bond length. Plotting this as a function of pressure reveals a continuous increase in coordination from 4 to 6 between 20 and 40 GPa (Meade *et al.* 1992) (figure 8). This change is responsible for the well-known high compressibility of glass at these pressures.

These results also provide insight into pressure-induced amorphization, a metastable transformation occurring in the solid state (i.e. below the melting tempera-

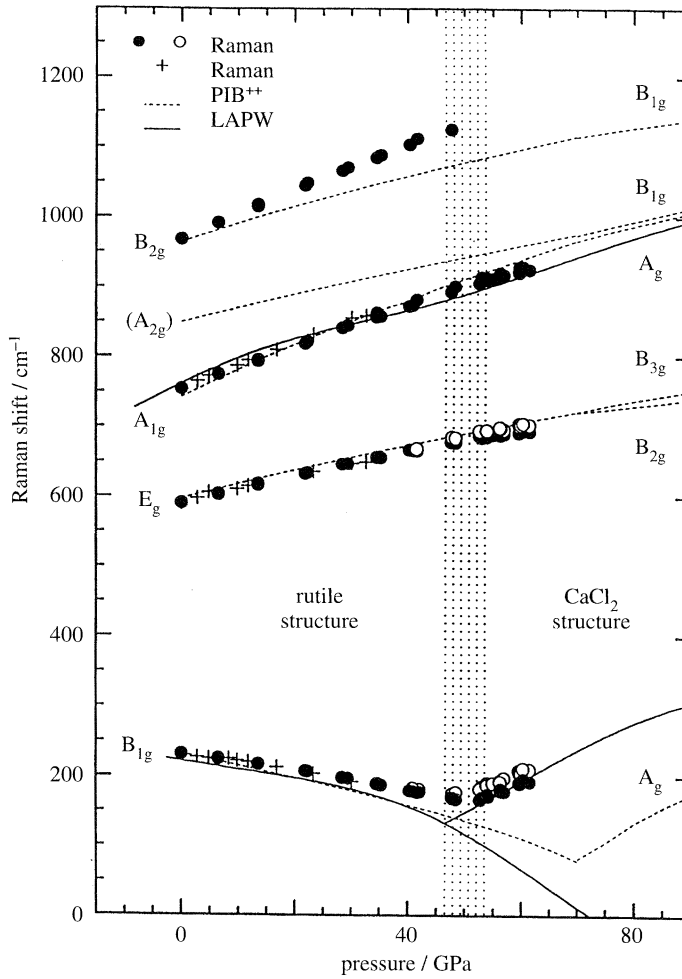

Figure 7. Pressure dependence of Raman frequencies for stishovite showing the transition from rutile-to-$CaCl_2$ transition (Kingma *et al.* 1995). The lines are the results of independent theoretical calculations.

ture). This was first documented in minerals for quartz and coesite (Hemley 1987). Crystals recovered from pressures of 25 GPa develop amorphous lamella seen as isotropic planar features (Kingma *et al.* 1993). Similar features are observed following shock metamorphism, both in laboratory and meteorite impact samples. In addition, X-ray diffraction measurements reveal a crystalline–crystalline transformation in the material. This occurs at about 21 GPa at room temperature, as shown by the appearance of new peaks in the powder diffraction pattern. With further increase in pressure, broad bands indicative of glass appear. In addition, intermediate crystalline–crystalline transitions associated with amorphization under pressure are now observed in coesite (Hemley 1987) and cristobalite (Palmer *et al.* 1994), and may in fact be a general phenomenon associated with such metastable transformations.

(*d*) (Mg,Fe)SiO_3 *perovskite*

The major role of (Mg,Fe)SiO_3 perovskite in the lower mantle is central to the prevailing paradigm of solid Earth geophysics. Detailed comparison between den-

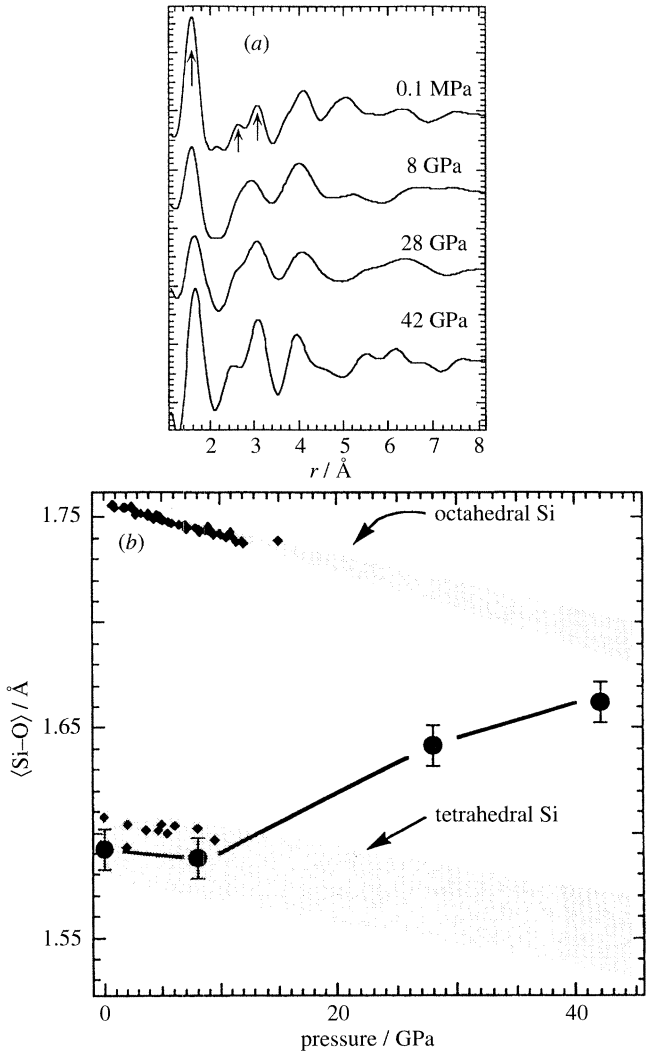

Figure 8. Effect of pressure on the local structure of SiO_2 glass (Meade *et al.* 1992). (*a*) Average pair-correlation function with increasing pressure obtained from the X-ray structure factor. (*b*) Si–O bond length as a function of pressure. The large circles correspond to the position of the first peak in (*a*); the small symbols are Si–O bond lengths from crystalline SiO_2 polymorphs, and the shaded bands show the estimated compressibility of each polyhedra.

sity and seismic parameters profiles obtained from mineral physics data with those determined by seismology indicate a high abundance of this phase (Stixrude *et al.* 1992). Such an analysis requires, however, some extrapolation of the experimental data using some form for the equation of state. At lower temperatures and at high pressures, the structure is orthorhombic, but whether or not this is the structure of silicate perovskite under the high P–T conditions of the lower mantle has been questioned; specifically, there is the possibility that the material undergoes a sequence of high-temperature transitions to higher symmetry forms (e.g. tetragonal, cubic) as is the case for other perovskite-structured materials (Hemley & Cohen 1992).

Figure 9 shows the electron density calculated from local density approximation/density functional methods for the cubic form (Hemley & Cohen 1992). The

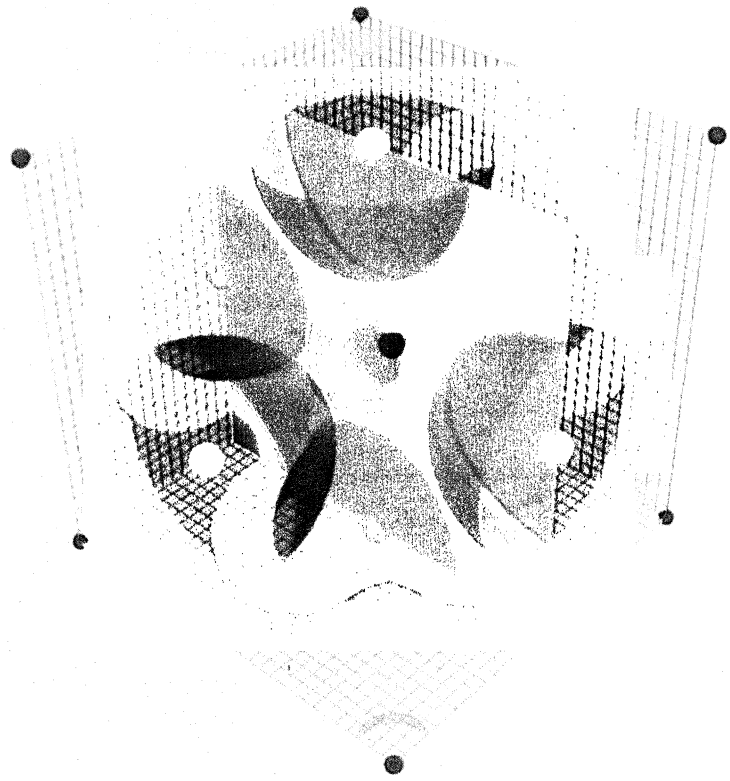

Figure 9. Charge density for cubic $MgSiO_3$ perovskite (after Hemley & Cohen 1992). The oxygens (on the faces) are fairly spherical, and there is a small amount of valence change on the Si. There is no valence charge on the Mg, which indicates that it is a fully ionized Mg^{+2} similar to that in MgO. Copyright Ronald E. Cohen.

shells of constant electron density are decidedly spherical, and the material is quite ionic. The distortions from cubic are classified in terms of the M- and R-point distortions. This has been examined theoretically in a large number of ionic model calculations during the past ten years (see, for example, Hemley & Cohen 1992). All of these studies agree that the orthorhombic form is stable at all pressures and at lower temperatures for the Mg-endmember. These methods, however, have been unable to provide quantitative predictions of structure and physical properties. More recently, this problem has been examined using more accurate theoretical techniques (Stixrude & Cohen 1993; Wentzcovitch *et al.* 1993). The energetics of octahedral rotation in the structure calculated by Stixrude & Cohen (1993) are shown in figure 10. This result is consistent with high P–T diamond-cell diffraction measurements (Mao *et al.* 1991) as well as the more recent higher temperature results (Funamori & Yagi 1993; Yagi & Funamori, this volume) for $MgSiO_3$.

The presence of Fe in magnesium-rich silicate perovskite can have important consequences for its chemical and physical properties. In fact, the chemistry of Fe has been controversial, in part because of the presence of both Fe^{+2} and Fe^{+3} in synthetic samples. There is now widespread evidence that Fe^{+2} in $(Mg,Fe)SiO_3$ substitutes for Mg in the larger A site (see Hemley & Cohen 1992). However, the Fe^{+3} may substitute in the smaller B (octahedral) site. In this regard, we note that an un-

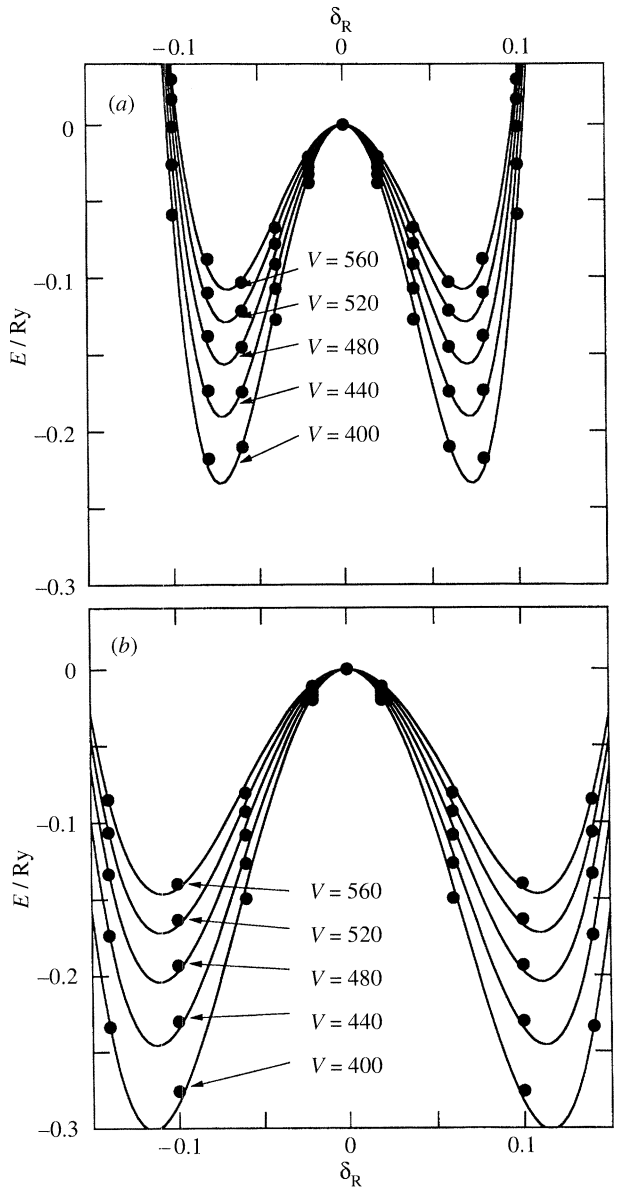

Figure 10. Energetics of octahedral rotations calculated for $MgSiO_3$ perovskite. LAPW total energies (10 atoms) relative to the cubic structure are plotted as a function of the M-point (a) and R-point (b) rotation angle, represented by the fractional change in the oxygen coordinate (Stixrude & Cohen 1993). Volumes are given in bohr^{-3}.

usual low-temperature electron delocalization transition has been observed recently by Mossbauer spectroscopy in samples containing both Fe^{+2} and Fe^{+3} (Fei *et al.* 1994). By simple ionic radius arguments, substitution of Fe for Mg will tend to stabilize cubic relative to the orthorhombic form because of the large size of the iron ion, although the larger size of Fe^{+2} seems insufficient by itself to stabilize the cubic structure. The existence of the high P–T cubic phase of $(Mg_{0.85}Fe_{0.15})SiO_3$ perovskite was suggested in a recent preliminary *in situ* synchrotron diffraction and CO_2

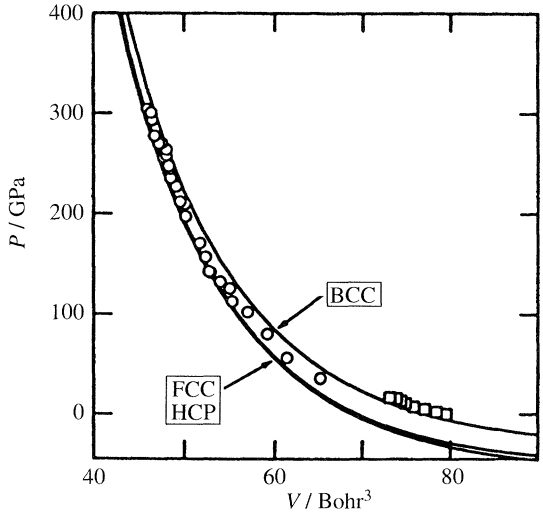

Figure 11. Room temperature pressure–volume equation of state for iron (see Mao *et al.* 1990) compared with the theoretical calculations with the generalized gradient approximation (Stixrude *et al.* 1994).

laser heating study (Meade *et al.* 1995); however, the results can also be explained by changes in sample texture and uncertainties in the volume of the sample being heated by the laser. This study reported high P–T dissociation of $(Mg_{0.86}Fe_{0.14})SiO_3$, but this is entirely consistent with the formation of the three phase assemblage $(Mg,Fe)SiO_3 + (Mg,Fe)O + SiO_2$ according to the known phase diagrams for this $Mg/(Fe + Mg)$ ratio (see Hemley & Cohen 1992).

(*e*) *Core materials*

The structure and equation of state of Fe and Fe-Ni have been determined by static compression X-ray diffraction techniques to 300 GPa (Mao *et al.* 1990). LAPW calculations carried out with the generalized gradient approximation (GGA) show excellent agreement with the experimental equations of state for both the BCC and HCP phases for iron over this pressure range (Stixrude *et al.* 1994) (figure 11). Moreover, these calculations find a high P–T BCC phase suggested for the inner core to be mechanically unstable (Stixrude & Cohen 1995*a*). Further, Stixrude & Cohen (1995*b*) have developed a new tight bonding model based on these LAPW calculations. This approach provides a straightforward way of calculating dynamical properties, such as elasticity. Stixrude & Cohen (1995*b*) have applied this to the issue of reported anisotropy of the inner core and have calculated forward models of the inner core from first principles. Plots of travel time anomalies as a function of the angle between the inner core ray segment and the Earth's spin axis for a angular source–receiver distance of 150° are consistent with HCP phase having a large degree of preferred orientation (c parallel to the Earth's spin axis). These predictions were made assuming a pure iron core (i.e. no alloying). The observation of the hexagonal NiAs phase of FeO and evidence for its metallic character provide a physico-chemical mechanism for incorporation of oxygen into the core. Another important light element to consider is hydrogen (Badding *et al.* 1991, 1992; Yagi *et al.* 1994). X-ray measurements to 60 GPa demonstrate that iron hydride is extremely stable relative to Fe and H.

3. Discussion

Recent experimental and theoretical studies reveal new insights into the evolution of structure and bonding with pressure in materials believed to comprise the Earth's deep interior. Striking effects of pressure are documented in some materials, such as the sequence of phase transitions in FeO. These changes can be understood from first-principles calculations but defy predictions based on simple models based on low-pressure data. On the other hand, rules developed for lower pressure phases can be used to predict the behaviour of other materials, such as MgO. For example, the concept of the ionic radius remains remarkably robust for materials which remain good insulators. However, accurate predictions require the inclusion of compressional effects on ion size as in the various non-empirical electron-gas calculations. Thus, sophisticated theories can be used to test simple rules for predicting structural changes in response to pressure and temperature, including phase transitions in crystals and amorphous phases.

Both increasing structural complexity and simplicity is observed with increasing pressure. For materials that have simple stoichiometries and remain insulators, the tendency toward close-packing results in structures generally becoming simpler at high pressures. For example, relatively complex lower-density crustal and upper-mantle minerals breakdown to assemblages containing simple oxides at very high pressures (i.e. B1, B2, or related structures), as pointed out by Birch (1952). On the other hand, compression of lower density structures can also produce the opposite effect: in quartz, the oxygens approach a close-packed substructure under pressure, but this leads to a lattice instability and amorphization. The distortion in stishovite from tetragonal to orthorhombic occurs because a higher packing efficiency for nearly spherical atoms is achieved by breaking the tetragonal symmetry with no deformation of the charge around the oxygen. The transition takes place because the oxygens in stishovite are far from being arrayed on a close-packed lattice. In this regard, we note that calculations suggest that compounds containing different sized atoms can exhibit surprisingly complex structures and phase diagrams, even for binary systems of particles interacting through simple (e.g. hard-sphere) interactions (Elkridge *et al.* 1992).

Changes associated with open-shell elements such as Fe are more significant and require more elaborate models to predict, particularly when band gaps close and the materials become metallic. Indeed, the high-pressure behaviour of mantle minerals containing open-shell elements may differ markedly from that of low-pressure (e.g. crustal) materials. With respect to the latter, it is interesting to note that there is evidence for new ordering schemes in majorite garnets (Hazen *et al.* 1994), and iron-bearing silicate spinels do not follow bulk modulus-volume systematics developed for low-pressure phases (Hazen 1993). Understanding the origin of pressure effects in metals generally requires consideration of compression effects on the band structure. These changes can be modelled using new tight binding schemes to calculate a wide variety of high P–T properties, as has been done for pure Fe (Stixrude & Cohen 1995*b*).

In this brief discussion, we have touched on pressure effects on selected end-member mantle and core phases. The effect of pressure-induced electronic transitions on solid solution behaviour is particularly significant. For example, it is important to examine the implications of the recently documented high-pressure transitions in FeO for the solid solution behaviour of (Mg,Fe)O. Magnesiowüstite forms a complete solid solution at low and moderately high pressure. However, it is not known if this persists

PHILOSOPHICAL TRANSACTIONS OF THE ROYAL SOCIETY A MATHEMATICAL, PHYSICAL & ENGINEERING SCIENCES

throughout the P–T range of the lower mantle, or if it will be limited to a relatively small range as it is in $(Mg,Fe)SiO_3$ perovskite. There is evidence for significant pressure effects on defect clustering and non-stoichiometry; this is particularly important for iron-bearing systems (e.g. Fe^{+3} $\square$). For example, nearly stoichiometric FeO can be formed only under pressure (see Fei & Mao 1994), but the fundamental basis for this is not understood. Furthermore the above results indicate that the concept of discrete valence may be ill-defined at high pressure, and pressure-induced changes in valence state may have significant effects on element partitioning at high pressure, possibly making extrapolations based on low-pressure data unreliable.

Finally, there is growing evidence for the large effect of pressure on chemical reactivity of volatiles. The formation of iron hydride under pressure is a compelling example of the large pressure effect on the reactivity of hydrogen and the stability of hydrogen-bearing phases under pressure. Recent work demonstrates that new stoichiometric dense hydrous silicates are stable to deep mantle pressures (see Farley 1995). Moreover, significant quantities of volatile components can be trapped in high-pressure phases, including hydrogen in nominally anhydrous minerals (Bell & Rossman 1991). Pawley *et al.* (1993) found that stishovite can hold significant amounts of hydrogen, and this is coupled with substitution of Al^{+3}. Similar results were obtained by Meade *et al.* (1994) for $MgSiO_3$ perovskite synthesized in H_2O. The stability of other volatile components in minerals at very high pressures, including binding of inert gases as found in low-Z ordered alloys (Vos *et al.* 1992), remains to be investigated. Each of these also remain challenges to theory.

We are grateful to H. K. Mao, L. Stixrude and T. S. Duffy for their contributions and many useful discussions regarding this work. Computing was performed at the National Center for Supercomputing Applications and the Pittsburgh Supercomputer Center. This research was supported by the NSF.

References

Badding, J. V., Hemley, R. J. & Mao, H. K. 1991 High-pressure chemistry of hydrogen in metals: *in situ* study of iron hydride. *Science* **253**, 421–424.

Badding, J. V., Mao, H. K. & Hemley, R. J. 1992 High-pressure crystal structure and equation of state of iron hydride: implications for the Earth's core. In *High pressure research: application to Earth and planetary sciences* (ed. Y. Syono & M. H. Manghnani), pp. 363–372. Tokyo: Terra; Washington, DC: American Geophysical Union.

Bell, D. R. & Rossman, G. R. 1991 Water in Earth's mantle: the role of nominally anhydrous minerals. *Science* **255**, 1391–1397.

Birch, F. 1952 Elasticity and constitution of the Earth's interior. *J. Geophys. Res.* **57**, 227–286.

Bukowinski, M. S. T. 1985 First principles equations of state of MgO and CaO. *Geophys. Res. Lett.* **12**, 536–539.

Bukowinski, M. S. T. 1994 Quantum geophysics. *A. Rev. Earth Planet. Sci.* **22**, 167–205.

Burdett, J. K. 1985 Electronic control of the geometry of rutile and related structures. *Inorg. Chem.* **24**, 2244–2253.

Causa, M., Dovesi, R., Pisani, C. & Roetti, C. 1986 Electronic structure and stability of different crystalline phases of magnesium oxide. *Phys. Rev.* B **33**, 1308–1316.

Cohen, R. E. 1991 Bonding and elasticity of stishovite SiO_2 at high pressure: linearized augmented plane wave calculations. *Am. Mineral.* **76**, 733–742.

Cohen, R. E. 1992 First-principles predictions of elasticity and phase transitions in high pressure SiO_2 and geophysical implications. In *High-pressure research: application to Earth and planetary sciences* (ed. Y. Syono & M. H. Manghnani), pp. 425–431. Tokyo: Terra; Washington, DC: American Geophysical Union.

PHILOSOPHICAL TRANSACTIONS OF THE ROYAL SOCIETY A MATHEMATICAL, PHYSICAL & ENGINEERING SCIENCES

Cohen, R. E. 1994 Theory of crystalline silica. In *Silica—physical behavior, geochemistry, and materials applications* Reviews of Mineralogy 29 (ed. P. J. Heaney, G. V. Gibbs & C. T. Prewitt), pp. 369–402. Washington, DC: Mineralogical Society of America.

Duffy, T. S., Hemley, R. J. & Mao, H. K. 1995 Equation of state and shear strength at multi-megabar pressures: magnesium oxide to 227 GPa. *Phys. Rev. Lett.* **74**, 1371–1374.

Elkridge, M. D., Madden, P. A. & Frenkel, D. 1992 Free energy calculations of simple two-component hard sphere systems. *Nature* **365**, 35–37.

Elsasser, W. M. 1951 Quantum-theoretical densities of solids at extreme compression. *Science* **113**, 105–107.

Farley, K. A. (ed.) 1995 *Volatiles in the Earth and Solar System.* New York: American Institute of Physics.

Fei, Y. & Mao, H. K. 1994 *In situ* determination of the NiAs phase of FeO at high pressure and temperature. *Science* **266**, 1678–1680.

Fei, Y., Virgo, D., Mysen, B. O., Wang, Y. & Mao, H. K. 1994 Temperature dependent electron delocalization in (Mg,Fe)SiO_3 perovskite. *Am. Mineral.* **79**, 826–837.

Funamori, N. & Yagi, T. 1993 High pressure and high temperature *in situ* X-ray observation of $MgSiO_3$ perovskite under lower mantle condition. *Geophys. Res. Lett.* **20**, 387–390.

Goldschmidt, V. M. 1926 Geochemische Verteilungsgesetze der Elemente, Skrifter Norske Videnskaps Akad Oslo I. Mat. Naturv. Klasse, Oslo.

Hazen, R. M. 1994 Comparative compressibilities of silicate spinels: anomalous behavior of $(Mg,Fe)_2SiO_4$. *Science* **259**, 206–209.

Hazen, R. M. & Finger, L. W. 1984 *Comparative crystal chemistry.* New York: Wiley.

Hazen, R. M., Downs, R. T., Finger, L. W., Conrad, P. G. & Gasparik, T. 1994 Crystal chemistry of Ca-bearing majorite. *Am. Mineral.* **79**, 581–584.

Hemley, R. J. 1987 Pressure dependence of Raman spectra of SiO_2 polymorphs: α-quartz, coesite, and stishovite. In *High-pressure research in mineral physics* (ed. M. H. Manghnani & Y. Syono), pp. 347–359. Tokyo: Terra; Washington, DC: American Geophysical Union.

Hemley, R. J. & Cohen, R. E. 1992 Silicate perovskite. *A. Rev. Earth Planet. Sci.* **20**, 553–600.

Hemley, R. J., Prewitt, C. T. & Kingma, K. J. 1994 High-pressure behavior of silica. In *Silica—physical behavior, geochemistry, and materials applications* (ed. P. J. Heaney, G. V. Gibbs & C. T. Prewitt). *Rev. Mineral.* **29**, 41–81. Washington, DC: Mineralogical Society of America.

Inbar, I. & Cohen, R. E. 1995 High pressure effects on the thermal properties of MgO. *Geophys. Res. Lett.* **22**, 1533–1536.

Isaak, D. G., Cohen, R. E. & Mehl. M. J. 1990 Calculated elastic and thermal properties of MgO at high pressures and temperatures. *J. Geophys. Res.* **95**, 7055–7067.

Isaak, D. G., Cohen, R. E., Mehl, M. J. & Singh, D. J. 1993 Phase stability of wüstite at high pressure from first-principles linearized augmented plane-wave calculations. *Phys. Rev.* B **47**, 7720–7731.

Jackson, I. & Ringwood, A. E. 1981 High-pressure polymorphism in iron oxides. *Geophys. Jl R. Astr. Soc.* **64**, 767–783.

Jeanloz, R. & Ahrens, T. J. 1980 Equations of state of FeO and CaO. *Geophys. Jl R. Astr. Soc.* **62**, 505–528.

Kingma, K. J., Cohen, R. E., Hemley, R. J. & Mao, H. K. 1995 Transformation of stishovite to a denser phase at lower mantle pressures. *Nature* **374**, 243–245.

Kingma, K. J., Meade, C., Hemley, R. J., Mao, H. K. & Veblen, D. R. 1993 Microstructural observations of α-quartz amorphization. *Science* **259**, 666–669.

Knittle, E. & Jeanloz, R. 1986 High-pressure metallization of FeO and implications for the Earth's core. *Geophys. Res. Lett.* **13**, 1541–1544.

Mao, H. K., Wu, Y., L. C. Chen, L. C., Shu, L. C. & Jephcoat, A. P. 1990 Static compression of iron to 300 GPa and $Fe_{0.8}Ni_{0.2}$ alloy to 260 GPa: implications for composition of the core. *J. Geophys. Res.* **95**, 21 737–21 742.

Mao, H. K., Hemley, R. J., Fei, Y., Shu, J. F., Chen, L. C., Jephcoat, A. P., Wu, Y. & Bassett, W. A. 1991 Effect of pressure, temperature, and composition on lattice parameters and density of (Fe,Mg)SiO_3-perovskites to 30 GPa. *J. Geophys. Res.* **96**, 8069–8079.

PHILOSOPHICAL TRANSACTIONS OF THE ROYAL SOCIETY A MATHEMATICAL, PHYSICAL & ENGINEERING SCIENCES

Mao, H. K., Shu, J. Hu, J. & Hemley, R. J. 1994 Single-crystal X-ray diffraction of stishovite to 65 GPa. *Eos* (Fall meeting suppl.) **75**, 662.

Mao, H. K., Shu, J. F., Fei, Y., Hu, J. & Hemley. R. J. 1996 The wüstite enigma. *Phys. Earth Planet. Inter.* (In the press.)

Meade, C., Hemley, R. J. & Mao, H. K. 1992 High-pressure X-ray diffraction of SiO_2 glass. *Phys. Rev. Lett.* **69**, 1387–1390.

Meade, C., Reffner, J. A. & Ito, E. 1994 Synchrotron infrared absorbance measurements of hydrogen in $MgSiO_3$ perovskite. *Science* **264**, 1558–1560.

Meade, C., Mao, H. K. & Hu, J. 1995 High-temperature phase transition and dissociation of $(Mg,Fe)SiO_3$ perovskite at lower mantle pressures. *Science* **268**, 1743–1745.

Mehl, M. J., Cohen, R. E. & Krakauer, H. 1988 Linearized augmented plane wave electronic structure calculations for MgO and CaO. *J. Geophys. Res.* **93**, 8009–8022.

Mehl, M. J., Hemley, R. J. & Boyer, L. L. 1986 Potential-induced breathing model for the elastic moduli and high-pressure behavior of the cubic alkaline-earth oxides. *Phys. Rev.* B **33**, 8685–8696.

Matsui, Y. & Tsuneyuki, S. 1992 Molecular dynamics study of rutile-$CaCl_2$ phase transition in SiO_2. In *High-pressure research: application to Earth and planetary sciences* (ed. Y. Syono & M. H. Manghnani), pp. 433–439. Tokyo: Terra; Washington, DC: American Geophysical Union.

Navrotsky, A & Davies, P. K. 1981 Cesium chloride versus nickel arsenide as possible structures for (Mg,Fe)O in the lower mantle. *J. Geophys. Res.* **86**, 3689–3694.

O'Keeffe, M. & Navrotsky, A. (eds) 1981 *Structure and bonding in crystals*, vols 1 and 2. New York: Academic.

Palmer. D., Prewitt, C. T. & Hemley, R. J. 1994 Raman spectroscopic study of high-pressure phase transitions in cristobalite. *Phys. Chem. Minerals* **21**, 481–488.

Pauling, L. 1927 The sizes of ions and the structure of ionic crystals. *J. Am. Chem. Soc.* **49**, 765–790.

Pauling, L. 1960 *The nature of the chemical bond.* Ithaca, NY: Cornell University Press.

Pawley, A. R., McMillan, P. F. & Holloway, J. R. 1993 Hydrogen in stishovite, with implications for mantle water content. *Science* **261**, 1024–1026.

Shannon, R. D. & Prewitt, C. T. 1969 Effective ionic radii in oxides and fluorides. *Acta Crystallogr.* B **25**, 925–946.

Sherman, D. M. 1991 The high-pressure electronic structure of (Mg,Fe)O: applications to the physics and chemistry of the lower mantle. *J. Geophys. Res.* **9**, 14 299–14 312.

Sherman, D. M. & Jansen, H. J. F. 1995 First-principles prediction of the high-pressure phase transition and electronic structrure of FeO: implications for the chemistry of the lower mantle. *Geophys. Res. Lett.* **22**, 1001–1004.

Stixrude, L. & Cohen, R. E. 1993 Stability of orthorhombic $MgSiO_3$ perovskite from first-principles calculations. *Nature* **364**, 613–616.

Stixrude, L. & Cohen, R. E. 1995*a* Constraints on the crystalline structure of the inner core: mechanical instability of BCC iron at high pressure. *Geophys. Res. Lett.* **22**, 125–128.

Stixrude, L. & Cohen, R. E. 1995*b* High pressure elasticity of iron and anisotropy of Earth's inner core. *Science* **267**, 1972–1975.

Stixrude, L., Hemley, R. J., Fei, Y. & Mao, H. K. 1992 Thermoelasticity of silicate perovskite and magnesiowüstite and stratification of the Earth's mantle. *Science* **257**, 1099–1101.

Stixrude, L., Cohen, R. E. & Singh, D. J. 1994 Iron at high pressure: linearized augmented-plane-wave computations in the generalized-gradient approximation. *Phys. Rev.* B **50**, 6442–6445.

Tsuchida, Y. & Yagi, T. 1989 A new post-stishovite high-pressure polymorph of silica. *Nature* **340**, 217–220.

Vos, W., Finger, L. W., Hemley, R. J., Hu, J., Mao, H. K. & Schouten, J. A. 1992 High-pressure van der Waals compound in helium–nitrogen mixtures. *Nature* **358**, 46–48.

Wentzcovitch, R. M., Martins, J. L. & Price, G. D. 1993 Ab initio molecular dynamics with variable cell shape: application to $MgSiO_3$. *Phys. Rev. Lett.* **70**, 3947–3950.

PHILOSOPHICAL TRANSACTIONS OF THE ROYAL SOCIETY A MATHEMATICAL, PHYSICAL & ENGINEERING SCIENCES

Wolf, G. H. & Bukowinski, M. S. T. 1988 Variational stabilization of the ionic charge densities in the electron-gas theory of crystals: applications to MgO and CaO. *Phys. Chem. Minerals* **15**, 209–220.

Yagi, T., Hishinuma, Yamaka, M., Uchida, T., Utsumi, W. & Fukai, Y. 1994 Formation and structure of iron hydride under the condition of the Earth's interior. In *High pressure science and technology—1993* (ed. S. C. Schmidt *et al.*), pp. 943–946. New York: American Institute of Physics.

Zhang, H. & Bukowinski, M. S. T. 1991 Modified potential-induced breathing model of potentials with closed-shell ions. *Phys. Rev.* B **44**, 2495–2503.

PHILOSOPHICAL TRANSACTIONS OF THE ROYAL SOCIETY A MATHEMATICAL, PHYSICAL & ENGINEERING SCIENCES

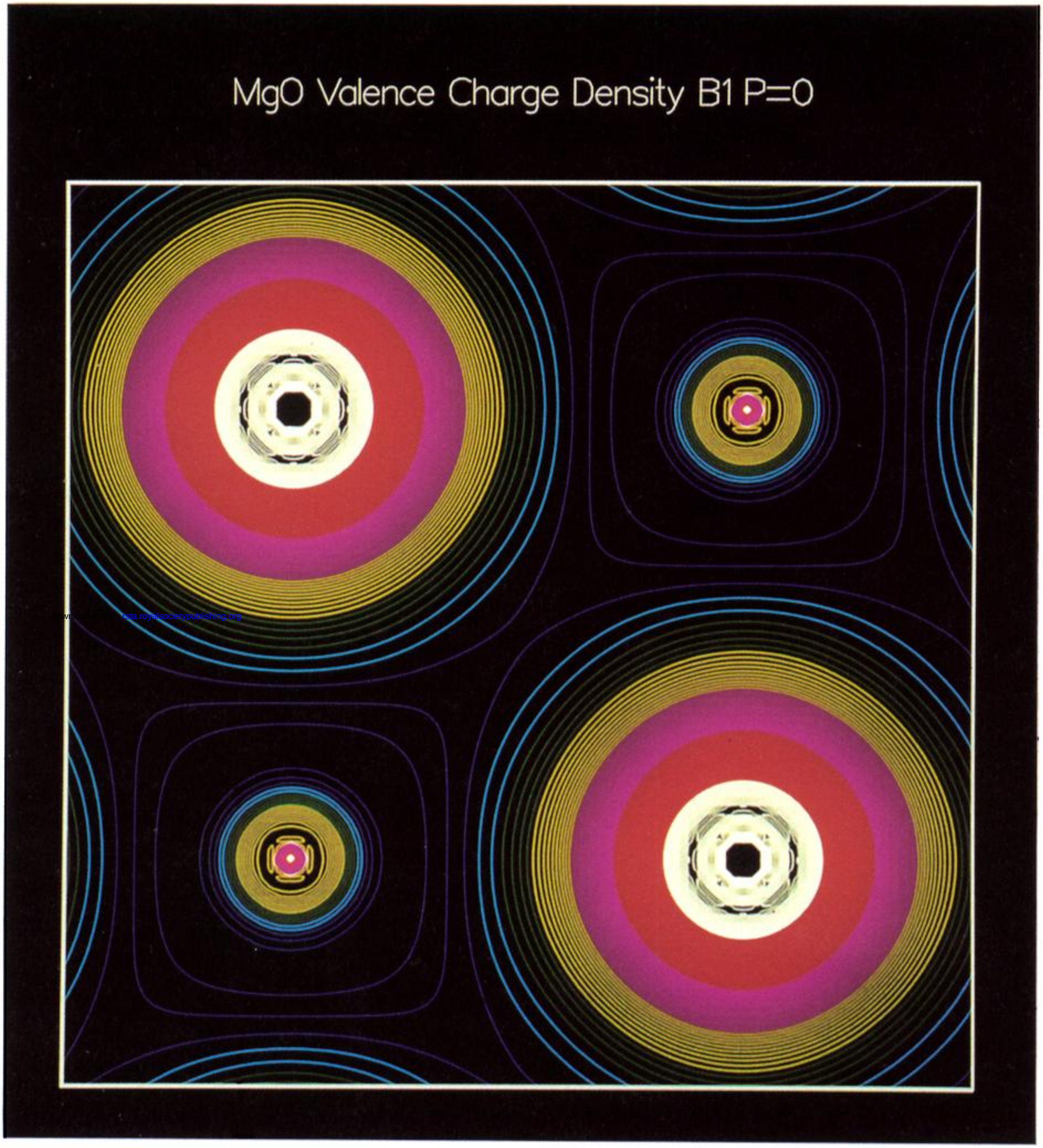

Figure 2. Calculated valence charge density contours for MgO in the B1 structure. (*a*) 5 GPa. (*b*) 754 GPa (Mehl *et al.* 1988). Only the O 2p states are shown. The contours correspond to 0.01 electrons bohr^{-3}. There is little valence charge on the Mg because of the highly ionic character of the material. However, MgO becomes less ionic at extreme conditions where more overlap is observed theoretically (*b*). In the higher pressure calculation, the B1 structure is metastable with respect to B2. Copyright American Geophysical Union.

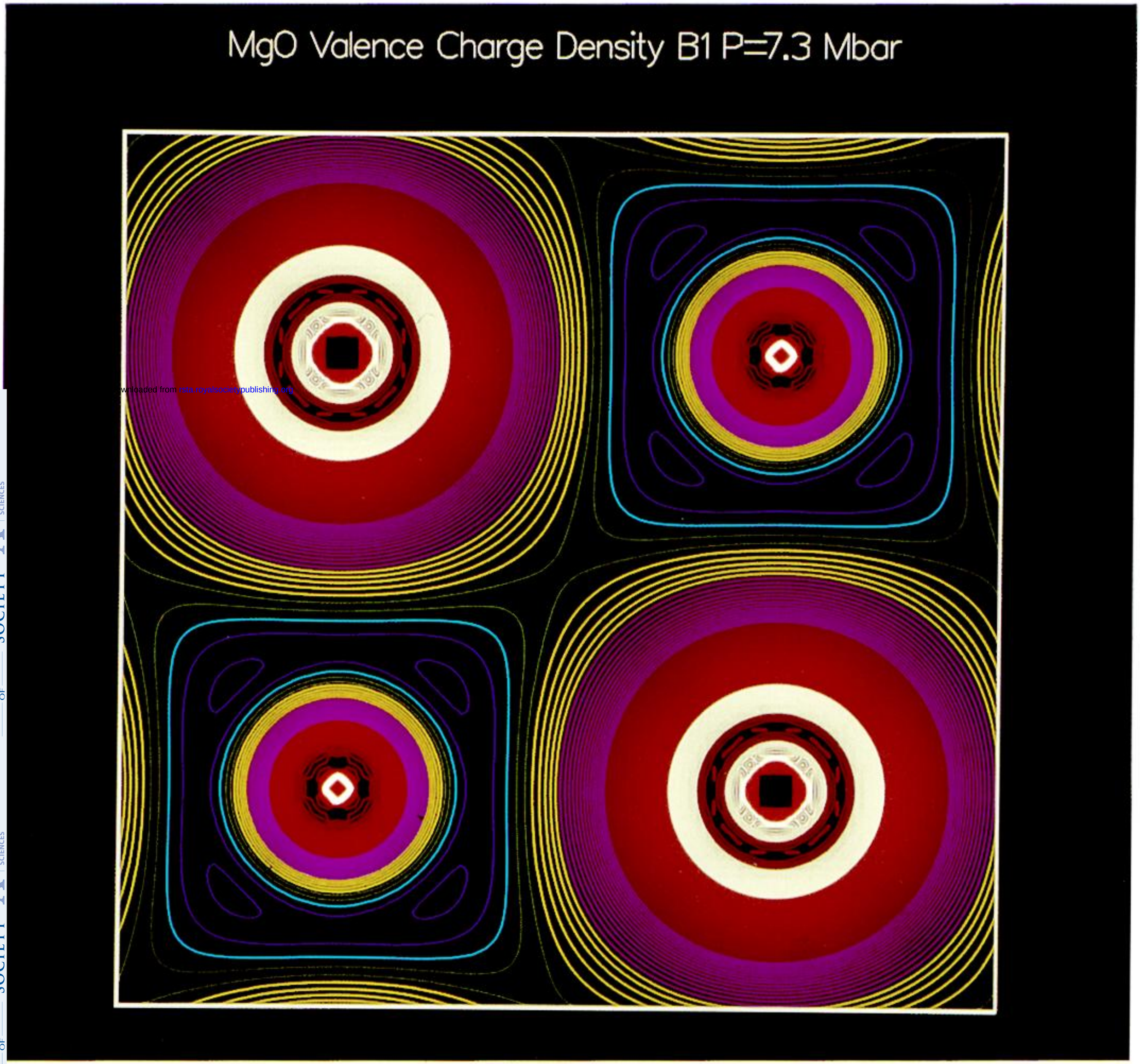

Figure 2. *Cont.*

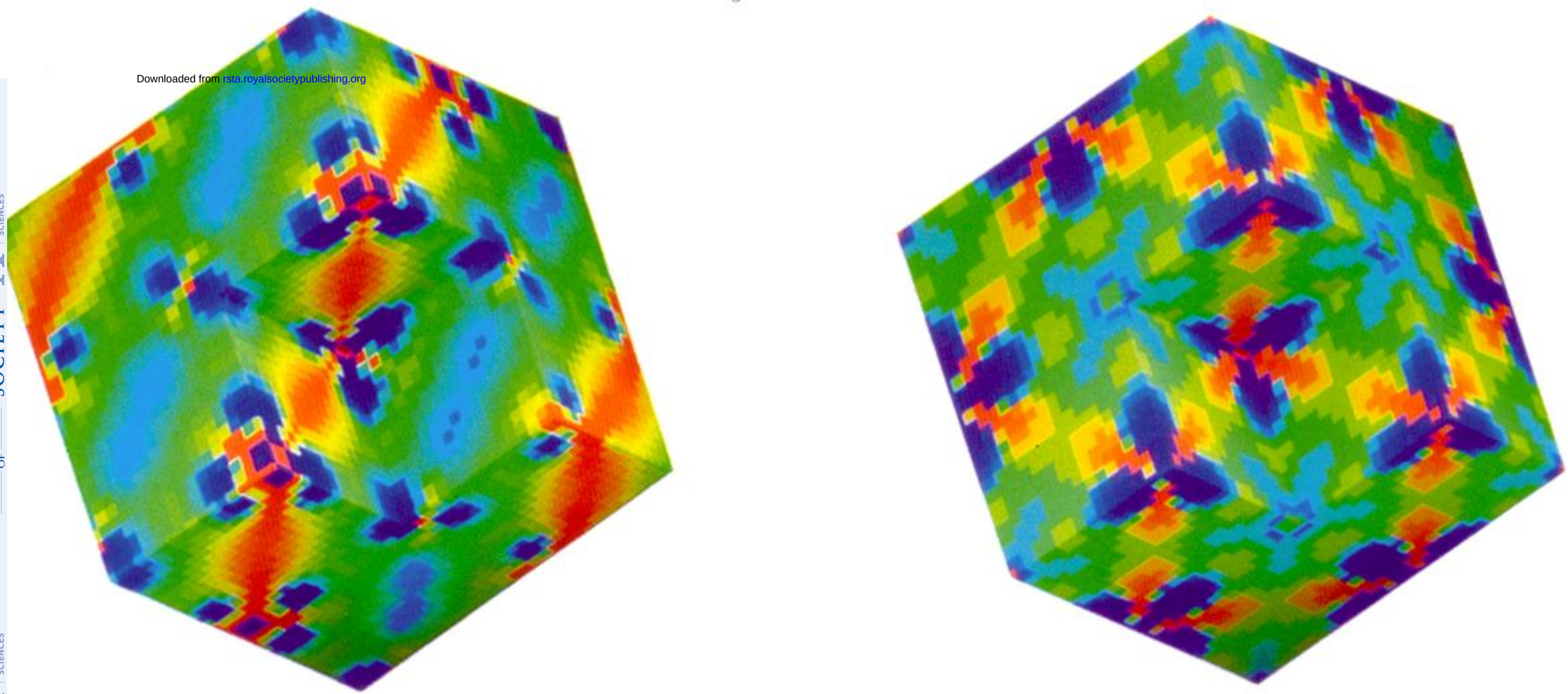

Figure 5. Difference charge density map for FeO between LAPW and PIB calculations. (*a*) Cubic (B1). (*b*) Rhombohedral strain (from Isaak *et al.* 1993). The Fe atoms are located at the centre of the cube and at the cube edges, and the O atoms are on the faces and corners. The red regions show excess charge relative to the spherical ions and the blue regions are deficient in charge. In the strained structure, there is pronounced metal–metal bonding shown by the red bands. Copyright Ronald E. Cohen.

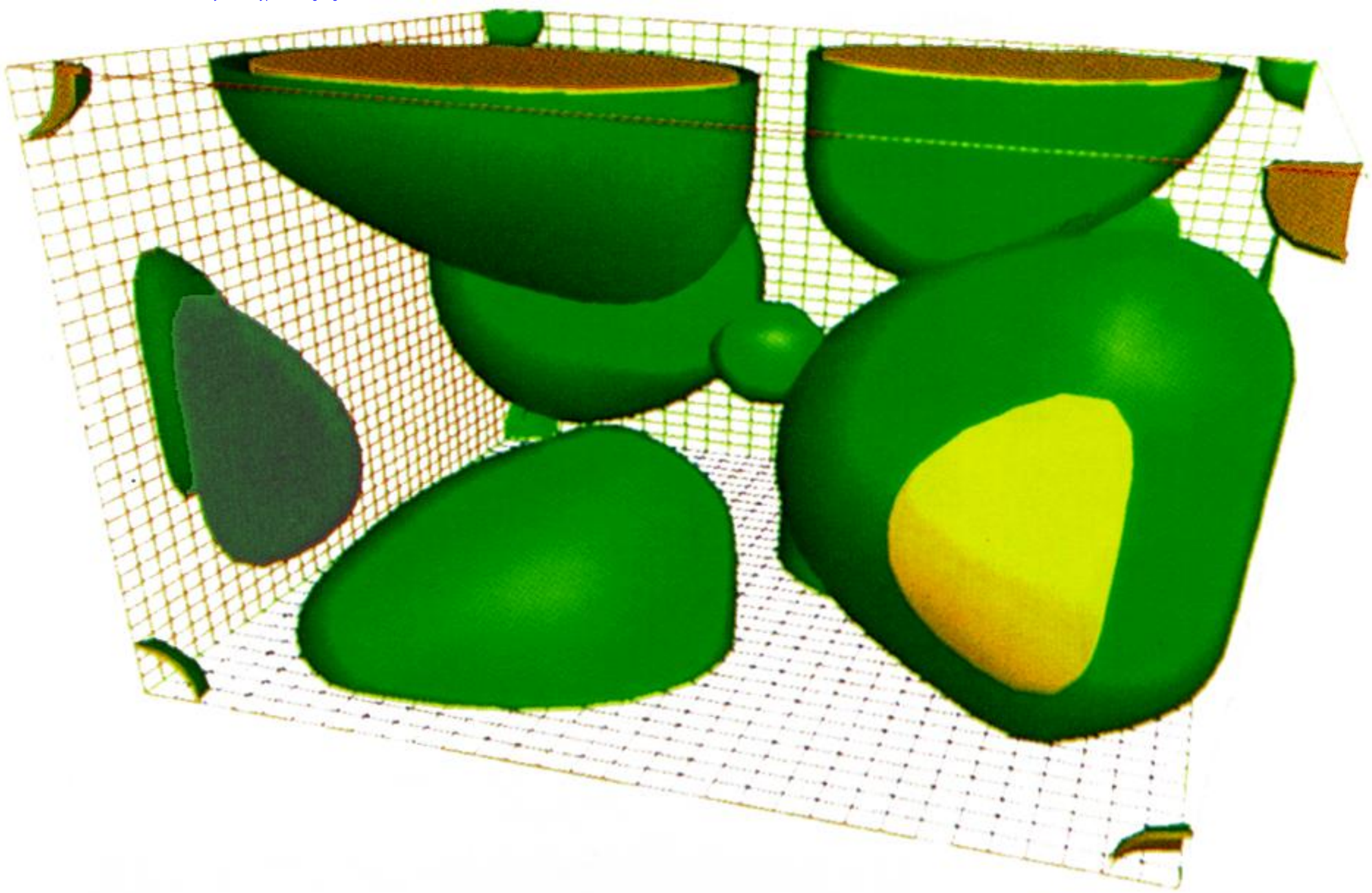

igure 6. Valence charge density surface for stishovite (from Cohen 1991, 1994). Two iso-density
ırfaces corresponding to 0.06 and 0.08 electrons bohr^{-3} are shown. Copyright Ronald E. Cohen.

PHILOSOPHICAL TRANSACTIONS OF THE ROYAL SOCIETY A MATHEMATICAL, PHYSICAL & ENGINEERING SCIENCES

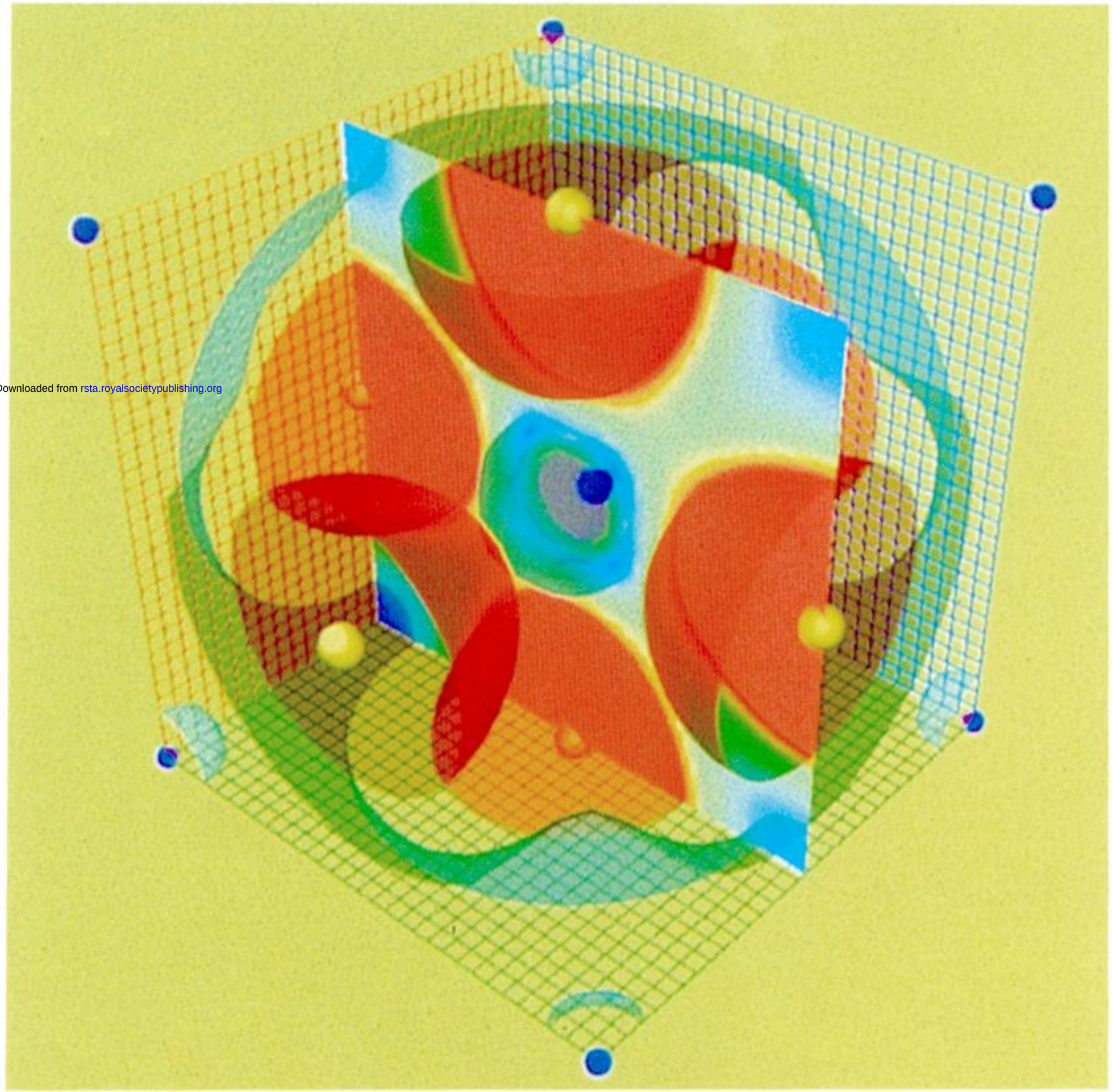

Figure 9. Charge density for cubic $MgSiO_3$ perovskite (after Hemley & Cohen 1992). The oxygens (on the faces) are fairly spherical, and there is a small amount of valence change on the Si. There is no valence charge on the Mg, which indicates that it is a fully ionized Mg^{+2} similar to that in MgO. Copyright Ronald E. Cohen.